CHAPTER 5
THE EFFECTS OF AUTOCLAVING TIMES AND TEMPERATURES ON PROPERTIES OF AAC INCORPORATING RHA

5.1 Introduction

As presented in the previous chapter, the introduction of aluminium powder played a crucial role in the properties of aerated concrete, which has an optimum dosage of 0.5% by weight of binder. Therefore, the mix proportion used as the reference in this chapter consists of 45% OPC, 5% CaO, 50% sand and the addition of aluminium powder of 0.5% by weight of binder. However, previous research studies have shown that the utilization of industrial by-products or waste residues, such as pulverised fuel ash, coal bottom ash and air-cooled slag, as cement replacement materials or as partial replacements for fine aggregates in AAC could enhance its properties in terms of density or strength [1, 4, 6, 7, 17]. In addition, this practice could reduce the amount of waste going into landfill as well as conserve the resource and save energy by means of decreasing the autoclaving time and temperature.

In Thailand, RHA is the most common agricultural waste [27, 56, 57] and has an effect on environmental pollution. However, it is well known that RHA has a high reactivity of silica, a high porous structure and low specific gravity [23, 56]. Thus, the application of RHA in aerated concrete greatly offers a potential solution by means of reducing waste into the ecosystem and enhancing the properties of aerated concrete. In this chapter, RHA was used as a silica source (sand) replacement at a level of 25-100% by weight for the investigation of reactive silica on the physical, mechanical structures and the microstructure of aerated concrete with and without autoclaved curing. Under autoclave conditions, the crystalline CSH, namely tobermorite, is most desirable for improving the strength of AAC, which could be synthesized at temperatures of 140-180°C at 12-24 h [19]. However, Taylor [21] recommended that each mix proportion has its own optimum autoclaving time and temperature, which if exceeded could lead to a decrease in strength. In addition, previous studies have reported that the reactivity of the silica source, the amount of Al added and the presence of alkali compounds strongly affected the formation of tobermorite [58, 59]. Therefore, autoclaved aerated concrete incorporating RHA was

also investigated for the effect of autoclaving temperatures and times, which was produced at temperatures of 140°C, 160°C and 180°C over different time periods.

5.2 Materials

The mixture of aerated concrete with RHA, called RHC, was produced from ordinary Portland cement (OPC), quick lime, quartz sand, RHA and water. The RHA used in this study was synthesised in a laboratory using an electric furnace at a temperature of 650°C for 1 h. It was then ground before being passed through sieve No. 325, with less than 34% by weight being retained, in accordance with ASTM C618 [48]. The crystalline phase of the RHA was analysed by X-ray diffraction (XRD; Miniflex using Cu Kα radiation (lλ = 1.5406 Å) at a voltage of 40 kV and 40 mA). Quartz sand was also ground to an average particle size of approximately 100 μm. Aluminium powder was provided by the Super Block Company, Limited. The physical properties of these materials are listed in Table 3.1 and 3.3.The chemical compositions of the materials used in this study were determined using X-ray fluorescence (XRF; WDXRF PW2400) analysis, and the results are provided in Table 3.2.

5.3 Experimental

The reference mix was composed of 45% OPC, 5% quick lime and 50% sand. The sand was replaced by RHA at levels of 25%, 50%, 75% and 100% to produce RHC25, RHC50, RHC75 and RHC100, respectively. Aluminium powder was added at 0.5% by weight of the binder (OPC + quick lime), and the water/binder ratio was determined by the flow table method to obtain a flow of 110±5% in accordance with ASTM C109 [49]. These mix proportions are summarised in Table 3.5. The solid components were mixed in a Hobart mixer for 1 min. Water was then added to the solid components, and the mixing was repeated for 1 min and 30 sec. This slurry was poured into 5 cm cubic steel moulds. After casting, the samples were preheated in an oven at 40°C for 3 h to achieve the desired setting and volume stability. The specimens were cured by normal curing at 7, 14 and 28 days and autoclave curing was conducted at three different temperatures: 140°C and 160°C for 4, 8 and 18 h, and at 180°C for 2, 4, 8 and 18 h.

After curing, the samples for compressive strength were dried at 40°C for 24 hr to remove the excess water in accordance with ASTM C1368 [60]. The remaining samples were dried at 105°C for 24 hr to determine their unit weights. After strength testing, the pieces of cracked samples were dried by soaking in acetone and used for microstructural analysis. The crystalline phases present in aerated concrete samples were observed using XRD technique at a step size 0.02°, scan rate of 3° per min and scan range of 10° to 60° 2θ. The morphology evolutions present in the samples were analyzed using SEM technique on gold-coated sections. Thermal conductivity was determined on 30×30×5 cm^3 RHC samples during autoclave curing for 8 hr in accordance with the ASTM C518 [51], Heat Flow Meter Method using the Thermal Conductivity of Building and Insulating Materials Unit B480.

5.4 Results and Discussion

5.4.1 The Crystallinity of RHA

The crystallinity of RHA is an important factor in the reaction with calcium hydroxide ($Ca(OH)_2$) for a pozzolanic reaction. This is because, if the silica oxide in RHA is crystalline, a pozzolanic reaction is slower than if the RHA were amorphous. From previous research, it was suggested that the amorphous state of silica oxide in RHA occurred by burning at temperatures between 200-800 °C [61, 62], and the phase transformation of RHA was found at a temperature of 760°C by differential thermal analysis (DTA) [63, 64]. According to research by Asawapisit *et al.* (2005) [65], which studied the proper burning conditions for high reactive rice husk ash, they reported that combustion at a temperature of 650°C for 1h was the optimum condition which had silica oxide (SiO_2) and soluble silica in sodium hydroxide (NaOH) at about 95.85% and 595.96 mg/g RHA, respectively. Therefore, in this research, RHA was prepared under this condition. The physical and chemical characteristics are given in Table 3.1 and 3.2, respectively, and the crystallinity of RHA was analyzed by using XRD, as shown in Fig 5.1.

The XRD technique was analyzed with CuKα, 40kv, 40mA and scanned at 2θ in the range of 10° to 100°. The results showed a broad peak of SiO_2, which can be seen at ≈

23° (2θ). This indicated that this silica was amorphous; including the silica content in the RHA which was about 92.7%, and was investigated by XRF.

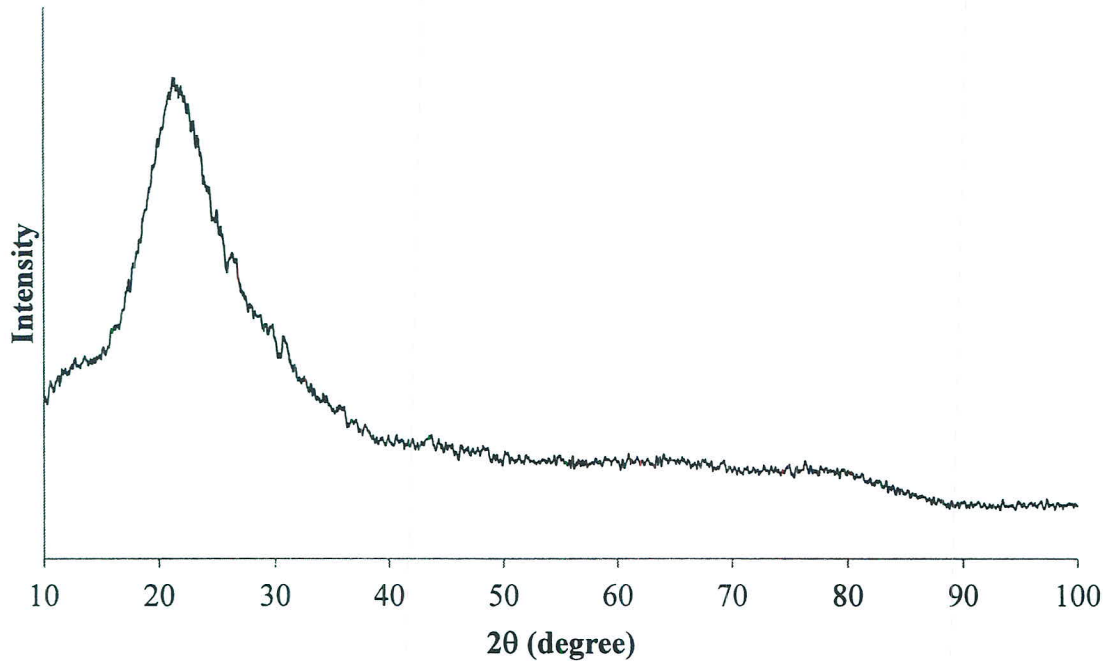

Figure 5.1 The XRD pattern of RHA.

5.4.2 The Effect of Curing Conditions

5.4.2.1 Compressive Strength

In construction buildings, autoclaved or high steam pressure curing is wildly would have in precast concrete due to faster building rates and lower shrinkage than normal curing. However, the disadvantage of high steam pressure is high energy consumption. In this study, the effect of curing conditions was also investigated in the aerated concrete incorporating RHA. The study was performed on non-autoclaved aerated concrete at 7, 14 and 28 days, as given in Fig. 5.2. It was found that the strength of all samples sharply increased in the early stage (7 days) and continued to increase until the 28th day. An increase in the strength of the samples occurred from the hydration reaction of the cement to produce calcium silicate hydrate (CSH) over time.

The introduction of RHA could be attributed to compressive strength reduction. This is because RHA is more porous and consequently required more water consumption to maintain workability, as given in Table 3.5. The other reason was that the hardness and the stiffness of RHA is weaker than of quartz sand. According to Chi *et al.* (2003) [66], it is recommended that the lower specific gravity of lightweight aggregate could be attributed

to compressive strength reduction. The strength loss compared to the control specimen, was calculated as 12, 33, 44 and 56% for RHA replacement ratios at 25, 50, 75 and 100%, respectively.

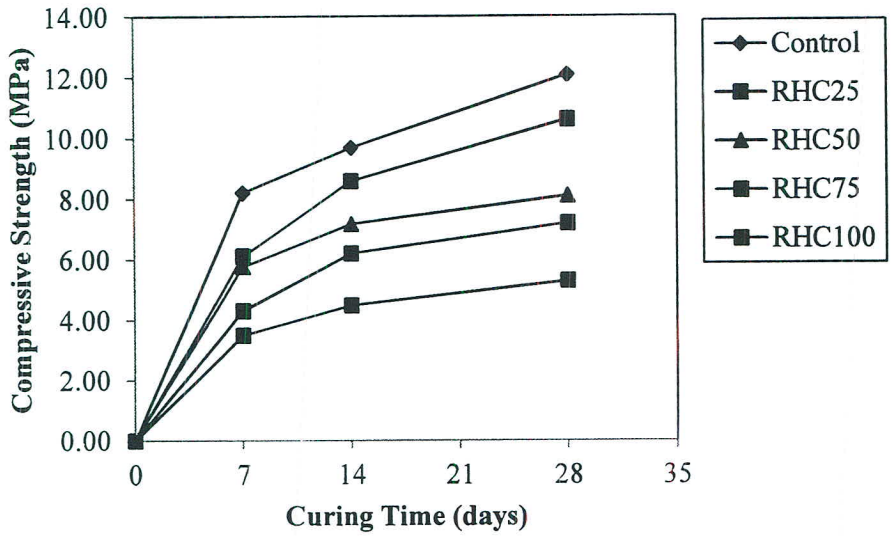

Figure 5.2 The compressive strength results of non-autoclaved aerated concrete.

In regards to the comparison curing conditions, the samples prepared by autoclave at 180°C for 8 hr were used to compare with the non-autoclaved samples at 28 days, as given in Fig. 5.3. Results indicated that at a mixture of up to 25% RHA replacement ratio, the autoclaved samples had relatively high strength than did the non-autoclaved samples. Concerning the reaction between the lime and quartz, it has a low degree of reaction due to quartz sand normally referred to low reactivity at normal temperature. However, thermodynamically, the increase in temperature represents an increase in the degree of reaction. This results in the dissolution of quartz which consequently rapidly reacts with the lime. Under high supersaturation, the nuclei and crystal growth is formed and transformed to the crystalline phase of calcium silicate hydrate, namely, tobermorite. Moreover, Taylor [21], also suggested that under hydrothermal treatment, the tobermorite is readily formed by using lime and finely ground quartz, but it is much less readily formed if amorphous silica is used. These reasons agree with the above findings in the high strength of autoclaved samples at low RHA replacement for sand.

In regards to the further RHA replacement ratio (over 25% RHA content), the autoclaved specimens present similar strengths to the non-autoclaved specimens.

Theoretically, the strength of the materials depends on the degree of the reaction. This indicates that the high reactivity of RHA promoted the high degree of pozzolanic reaction in normal curing at 28 days. Such reaction also increases CSH gel from the reaction between lime and amorphous silica in RHA as the hydrothermal reaction from lime and quartz.

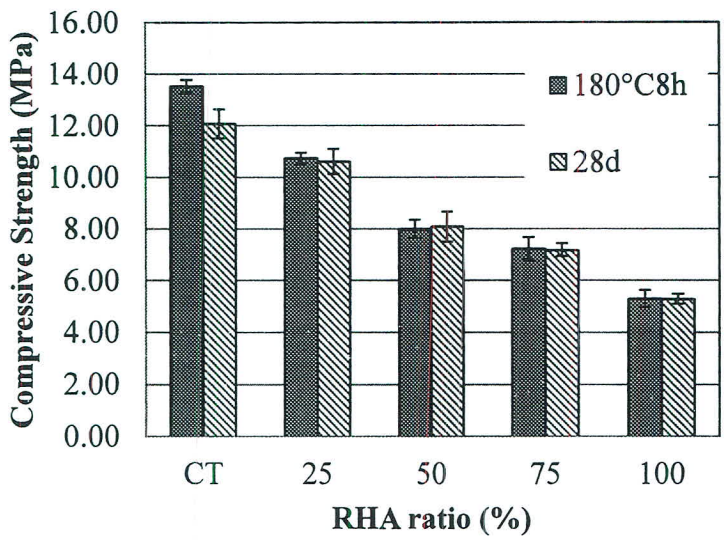

Figure 5.3 The effect of curing conditions on compressive strength.

5.4.2.2 Dry Density

Fig 5.4 shows the effect of curing conditions on the dry density of RHC samples. The dry density of aerated concrete is reduced when RHA is present. This is because of the relatively lower specific gravities (2.13) and the pore structure of RHA compared to sand (2.59) which could be attributed to these dry density reductions. Kurama *et al.* (2009) [1] and Karakurt *et al.* (2010) [4] also found that the constitution of low specific gravity and pore structure of residues can decrease the dry density of aerated concrete. However, the particle size also has an effect on dry density, according to Wongkeo and Chaipanich (2010) [6], in which they used coal bottom ash (specific gravity is 2.5) to replace OPC (specific gravity is 3.15) and reported that the dry density increased with the increasing amount of coal bottom ash. This was because of a finer particle size of coal bottom ash (7.81 μm) than OPC (8.31 μm) which lead to a greater arrangement of particles and a reduction of voids in the samples.

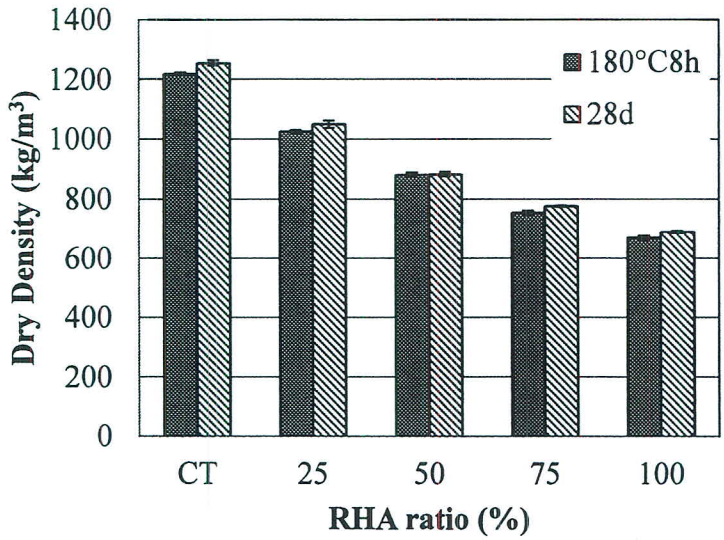

Figure 5.4 The effect of curing conditions on dry density.

As in the comparison of curing conditions, the dry density of aerated concrete became stable or changed slightly over a longer autoclaving time, as given in Fig 5.4. It can be concluded that the dry density decreased or increased depending on the starting materials and the mix proportion. From the previous research studies, it has been recommended that the density or pore structure of aerated concrete mostly occurs from the reaction between metallic aluminium and calcium hydroxide or alkali [6, 18, 54], as shown in Equation 1.1. However, such reaction is also involved with the composition parameters, especially water and lime. A lesser water-solids ratio could be attributed to insufficient aeration [18]. Similar results were reported by Cabrillac *et al.* (2006) [54], the pore structure depended on the presence of water and lime in the composition: the high water with lime could reduce density, but it does not influence the introduced porosity in the absence of lime. However, in this study, the water content was high because of the need to maintain workability. Therefore, this effect has no consideration. The mostly dry density reduction of RHC samples compared to the control sample was influenced by the RHA as the sand replacement.

$$2Al + 3Ca(OH)_2 + 6H_2O \rightarrow 3CaO{\cdot}Al_2O_3{\cdot}6H_2O + 3H_2 \qquad (1.1)$$

5.4.2.3 Microstructures

In this study, the microstructure of the final products was investigated using XRD combined with SEM analysis, which determined the samples prepared from normal curing for 28 days and autoclaved at 180°C for 8 h. In regards to the control sample prepared for 28 days, a high intensity of quartz and subsequent CSH, $Ca(OH)_2$ peak was found. However, the samples prepared from autoclaving conditions led to a decrease in the $Ca(OH)_2$ peak in the control samples and an increase in CSH crystalline, namely tobermorite, as shown in Fig. 5.6. This indicated that the hydrothermal treatment accelerates the reaction of lime and quartz to generate a crystalline CSH [67]. The sand substituted by RHA causes the $Ca(OH)_2$ peak to disappear and a total loss of the quartz peak in 100% RHA content in both conditions. Moreover, the introduction of RHA in the autoclave samples also found the tobermorite peak at all mix proportions.

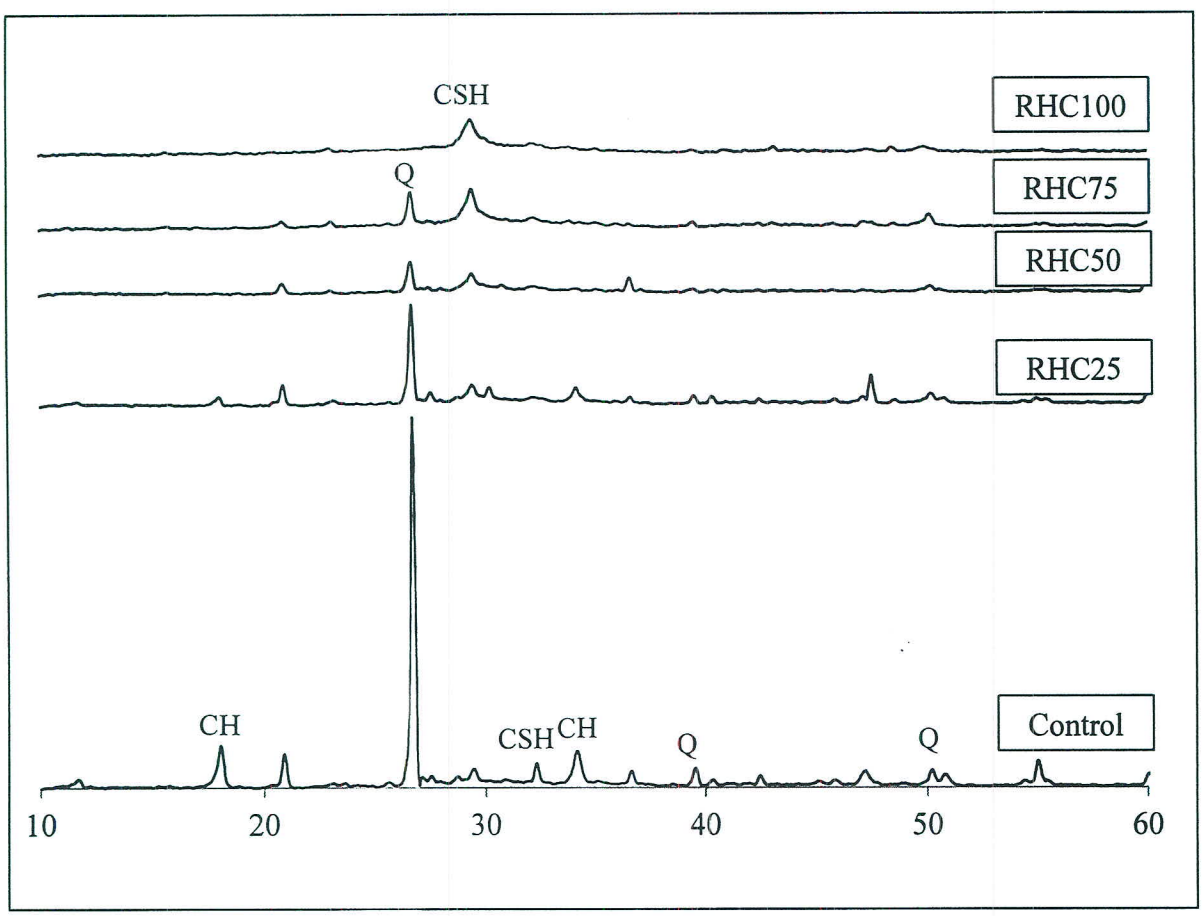

Figure 5.5 XRD pattern of aerated concrete at 28 days. CSH: calcium silicate hydrate; CH: calcium hydroxide; Q: quartz.

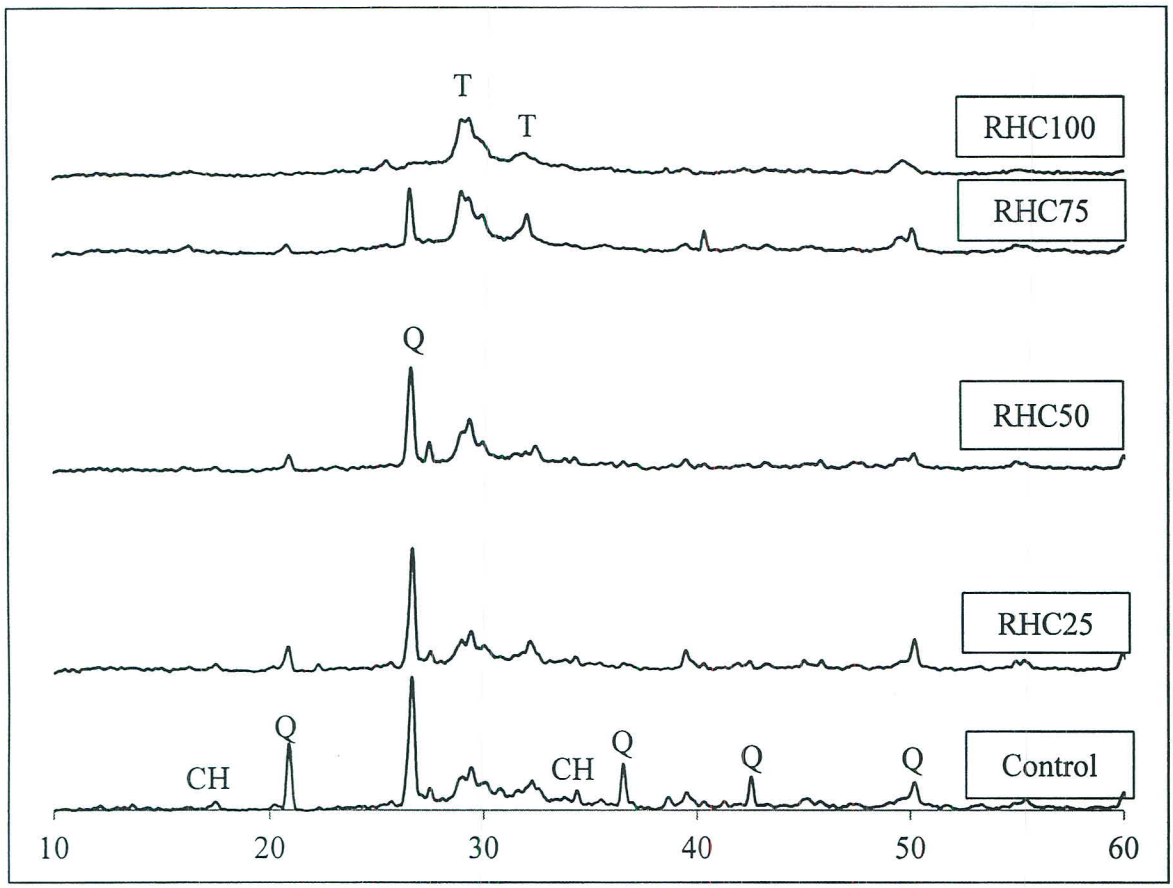

Figure 5.6 XRD pattern of autoclaved aerated concrete at 180°C for 8 hr. T: tobermorite; CH: calcium hydroxide; Q: quartz.

Regarding SEM analysis, at normal curing for 28 days, in the reference samples fibrous CSH, $Ca(OH)_2$ plate and ettringinte was found on the surface (Fig. 5.7a). The presence of RHA brings the disappearance of $Ca(OH)_2$ plate and only fibrous CSH was found (Fig. 5.7b-c). An increase in RHA content resulted in more RHA residues on the surface (Fig. 5.7d-e) and consequently compressive strength reduction. The change in condition (autoclave curing), initially found needle tobermorite (Fig. 5.8a) which changed to platy tobermorite when RHA was introduced (Fig 5.8b-c). With further RHA replacement ratio, crumbled foiled tobermorite is formed and transformed to glass-like structure CSH with very low Ca/Si ratio once 100% RHA content is reached. This finding is in agreement of XRD pattern in terms of the reduction of $Ca(OH)_2$ and the increase of CSH crystalline in hydrothermal treatment. Moreover, in the samples prepared from high steam pressure ettringite was not found because of the decomposition of CAH phase at temperatures of 70-100°C [21].

In the considerable hydration reaction, the cement hydration products at an ambient temperature are the amorphous CSH and $Ca(OH)_2$, which continue to react over time. However, the utilization of pozzolanic materials, such as fly ash, silica fume as well as RHA, tend to decrease $Ca(OH)_2$ and form CSH gel at a later stage [8]. This phenomenon has a strong effect on strength improvement. On the other hand, using pozzolanic materials over the limits gave a negative effect on strength due to the unreacted residues. In autoclave curing, a high temperature causes the dissolution of silicate anions from quartz resulting in a reduction in the Ca/Si ratio. At low Ca/Si ratios (0.8-1.0) and high temperatures (above 140°C) [19, 45], the amorphous CSH is transformed to tobermorite crystalline and gives high strength with shorter operation times (less than 24 hr) compared with normal curing (28 days). However, Taylor [21], also suggested that each mix proportion or each starting material had its own optimum autoclaving time and temperature, which if exceeded could lead to a decrease in strength.

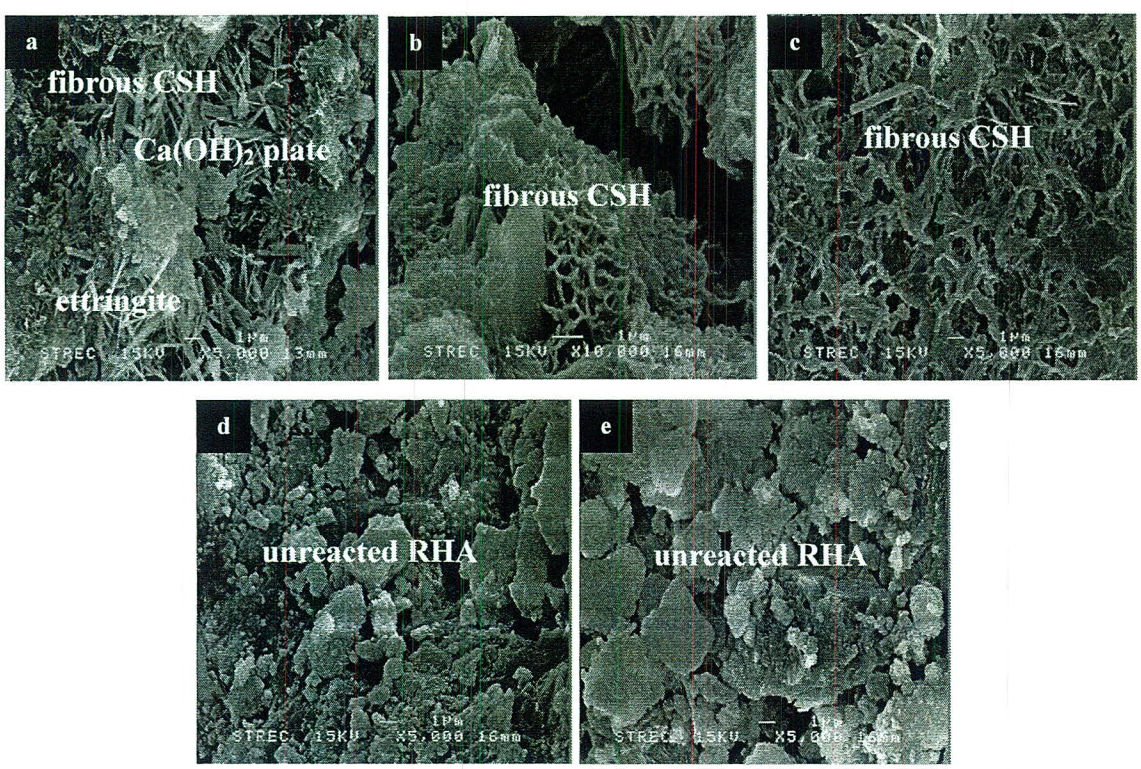

Figure 5.7 The morphology of aerated concrete at 28 days: (a) control, (b) RHC25, (c) RHC50, (d) RHC75 and (e) RHC100.

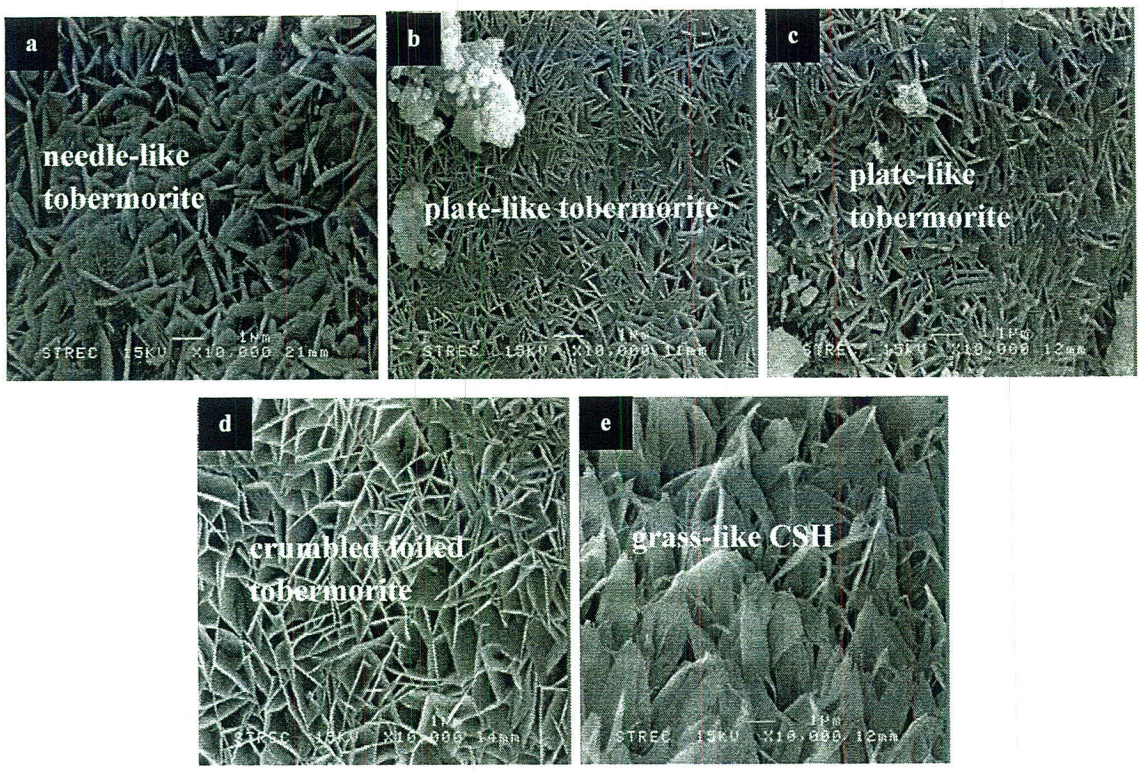

Figure 5.8 The morphology of autoclaved aerated concrete at 180°C for 8 hr: (a) control, (b) RHC25, (c) RHC50, (d) RHC75 and (e) RHC100.

5.4.3 Effect of Autoclaving Temperature and Time

In this study, the effect of autoclaving temperature and time on the final AAC products was tested at 180°C for 2, 4, 8 and 18 hr, and at both 140°C and 160°C for 4, 8 and 18 hr. The compressive, dry density and microstructure were investigated.

5.4.3.1 Compressive Strength

At a high temperature (180°C), the control and 25% RHA substitution for sand mixtures increased rapidly in strength during 2 hr autoclaving time and a slow increase with further autoclaving time, as given in Fig 5.9. This is because both mixtures contained high concentrations of quartz sand. It is well known that an increase in the degree of the reaction of quartz sand is done by increasing the temperature over time [68, 69]. This has a strong effect on the reaction of lime and quartz with the progress of time and corresponds to strength improvement. In the over 25% RHA substitution for sand, the compressive strength also sharply increased at 2 hr autoclaving time but became constant after 4 hr autoclaving time. This is because amorphous silica (RHA) still has a relatively high degree of reaction compared to quartz at the same temperature [70], and results in the rapid

consumption of lime to generate hydration products in shorter autoclaving times. The existence of such a reaction is supported by the finding that the compressive strength for RHA replacements greater than 50% remained stable even after further curing. This suggests that the utilization of pozzolanic residues could be attributed to a reduction in autoclaving time or temperature.

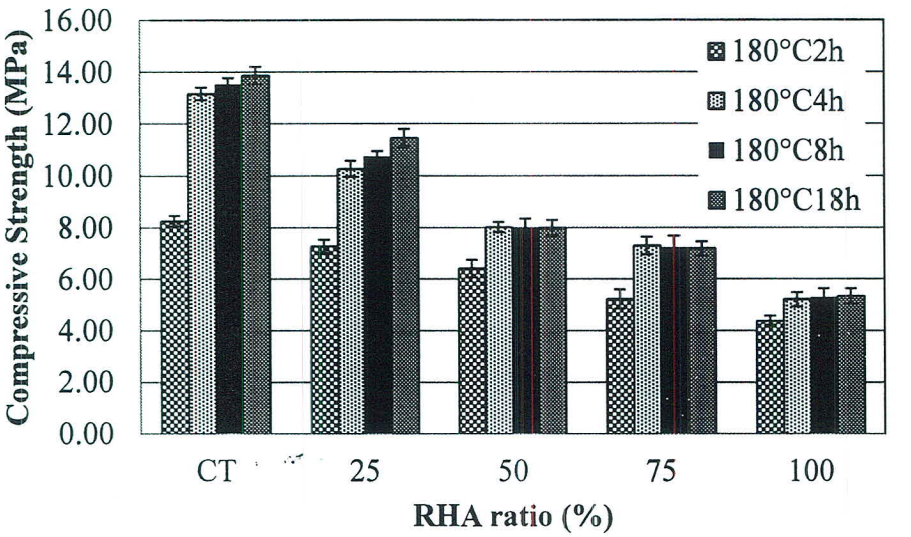

Figure 5.9 The compressive strength results of final AAC products at 180°C.

Fig. 5.10 shows the compressive strength results of the final AAC products at 160°C at various times. It was found that the compressive strength of all mix proportions also decreased with an increase in RHA content; however, the compressive strength increased with an increase in autoclaving time. Similarly, the low autoclaving temperature (140°C) produced an increase in compressive strength with the further autoclaving time, as given in Fig. 5.11. Only the mix proportions with 75% of RHA substitution at different temperatuers and times are shown in Fig. 5.12, this indicated that the strength of the samples from a high temperature (180°C) at all times gave relatively high strength compared with the other temperatures tested. However, the samples prepared with a long autoclaving time (18 hr) at 160°C gains nearly compressive strength with the sample prepared at temperature of 180°C.

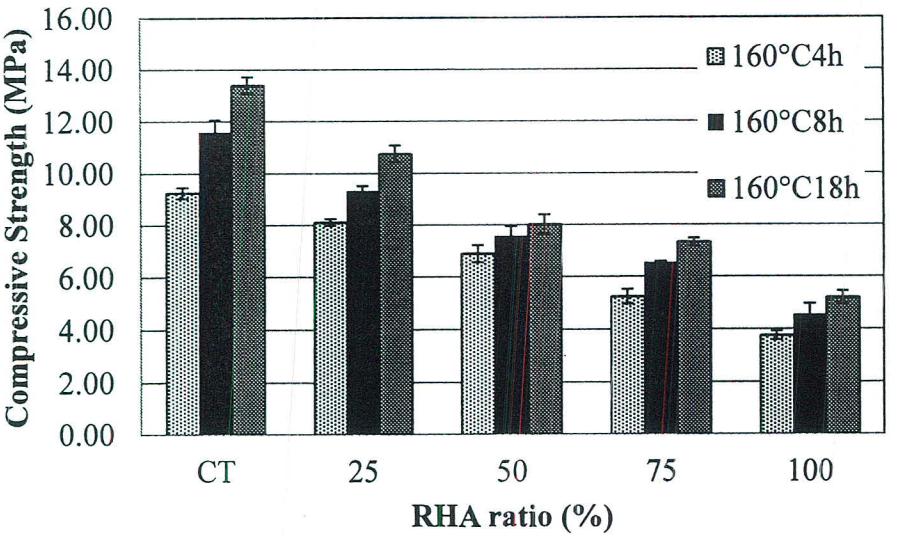

Figure 5.10 The compressive strength results of final AAC products at 160°C.

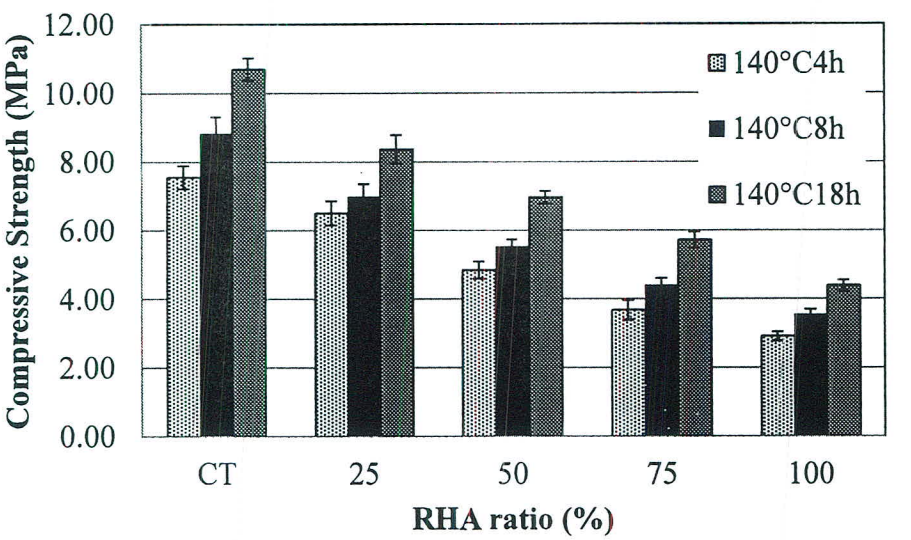

Figure 5.11 The compressive strength results of final AAC products at 140°C.

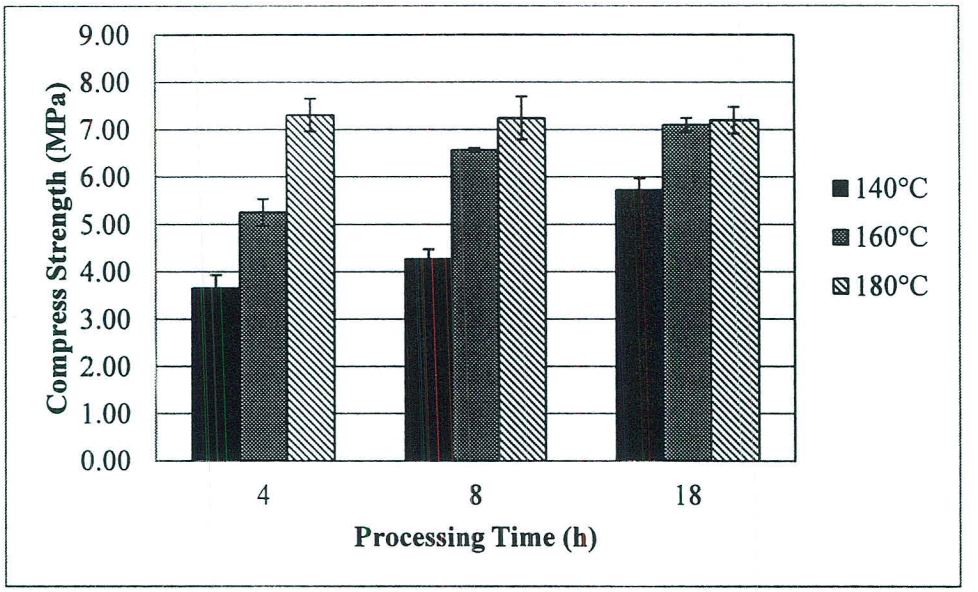

Figure 5.12 The effect of autoclaving temperatures and times of RHC75 on compressive strength.

In thermodynamics, the degree of reaction or entropy depends on temperature, pressure and phases. It is well known that an increase in temperature can enhance entropy in all phases. Thus, the use of autoclaved curing in this thesis leaded to increase the entropy of materials, such as RHA and quartz sand, and hydration products, such as CSH, in which corresponded with the dissolution of silicate anions and metastable phases, respectively. This phenomenon plays significant role on formation of tobermorite and the development of strength of AAC. The previous research reported that the formation of tobermorite proceeds via three step [67, 71, 72]; (1) the initially formed fibrous Ca-rich CSH aggregate and $Ca(OH)_2$ from the hydrated reaction of C_2S or C_3S during the molding process. With an increase in temperature by autoclaved conditions, silicate anions are dissolved from the quartz reducing the Ca/Si ratio, which rapidly react with Ca-rich CSH and $Ca(OH)_2$ to form crystallized tobermorite. When the reaction time is prolonged, the highly crystalline tobermorite is retarded and some quartz remains as an unreacted residue. This reaction is summarized in Equation 5.1.

$$\text{CSH or } Ca(OH)_2 + \text{silicate anions} \rightarrow \text{tobermorite} \qquad (5.1)$$

In theory, the tobermorite forms at Ca/Si ratio of 0.8-1.0 and temperatures of 140-200°C. Above these temperatures, it transforms to xonotlite ($Ca_6Si_6O_{17}(OH)_2$), which produces a weak crystalline structure. From the above mentioned, at the lowest temperature (140°C) of this study, the rate of dissolution of silicate anions was relatively slow compared with a temperature of 160°C or 180°C. This phenomenon also relates with the concentration of the Ca/Si ratio in the system. Therefore, the slow rate of silica dissolution leads to a longer time period for the optimum yield of Ca/Si ratio on tobermorite formation, which increases the strength with a longer autoclaving time.

5.4.3.2 Dry Density

Dry density has also decreased with an increasing RHA content and was stable or slightly changed even though the autoclaving time increased, as shown in Fig. 5.13. A slight increase in the dry density of some of the mixtures (RHC25, RHC75 and RHC100) was observed when the duration of autoclaving was extended to 18 hr, and this might be due to the formation of more solid hydration products in the concrete. Considerable phase evolution occurred during the AAC processing; the cement phases, mainly alite (C_3S) and belite (C_2S), were transformed into CSH phases and $Ca(OH)_2$ during the moulding process. Under high steam pressure, the silica in the quartz is dissolved and rapidly reacts with CSH and $Ca(OH)_2$ to form tobermorite or other products, such as xonotile (C_6S_6H) or α-dicalcium silicate hydrate, depending on the starting materials and the duration and temperature of the autoclaving step. At this stage, the hydration products form as autoclaving progresses. In addition, an earlier study performed by Taylor [21] demonstrated that the unit weight of the hydration products was in the range of 2200-2500 kg/m^3 (for example, CSH = 2250 kg/m^3 and 1.1 nm tobermorite = 2481 kg/m^3). This result indicated that autoclaving for a longer time leads to a decrease in the porosity and unit weight of the AAC produced [52].

In regards to the effect of autoclaving temperature, the RHC75 mixture was used to explain this observation, as shown in Fig.5.14. It shows that dry density was also still found to be stable at a short processing time for all temperatures, but slightly increased as autoclaving time progressed. This implied that dry density depended on the starting materials and the expansion reaction of metallic aluminium with alkali or $Ca(OH)_2$. The dry density loss of the RHC samples compared with the control samples was in the range of 16-45% for the samples that were subject to 8 hr and 18 hr of autoclave curing.

Moreover, upon comparison of the dry density and compressive strength results of this study with the ASTM C1386 standard [60], it was observed that the properties of the RHC75 and RHC100 samples autoclaved at 180°C for 4 hr and 160°C for 18 hr had exceeded the standard values. RHC75 exceeds AAC-6 (minimum strength is 6 MPa, unit weight limit is 750-850 kg/m^3) and RHC100 exceeds AAC-4 (minimum strength is 4 MPa, unit weight limit is 650-750 kg/m^3).

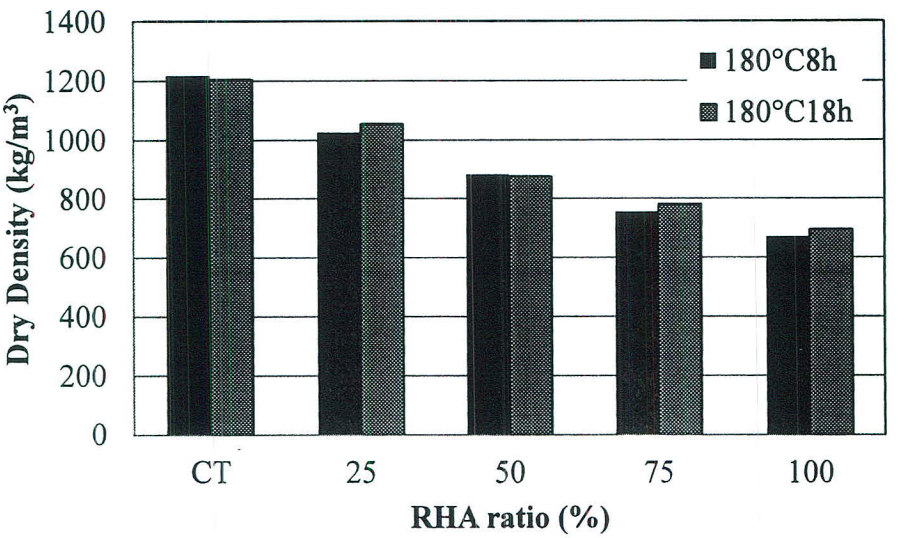

Figure 5.13 The effect of autoclaving time on dry density.

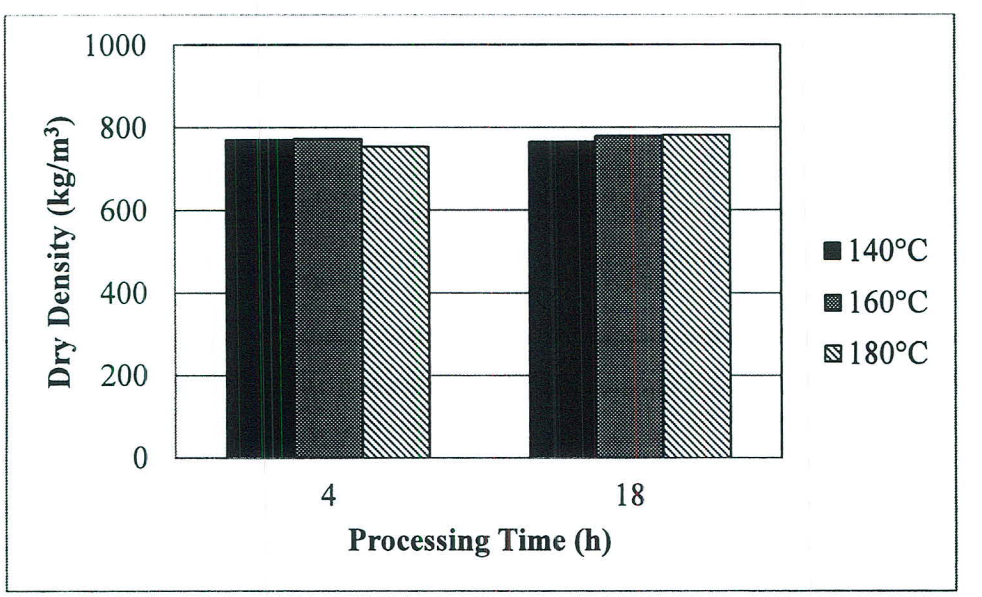

Figure 5.14 The effect of autoclaving temperatures and times of RHC75 on dry density.

5.4.3.3 Thermal Conductivity

Typically, the thermal conductivity of AAC depends on the density, moisture content and the starting materials used in the AAC process, including the pore fraction and distribution [18]. In this study, all mixtures at 8 hr of autoclaving time were used to determine the thermal conductivity values, and these are provided in Table 5.1. The results indicate that the thermal conductivity of RHC decreased as the RHA dosages increased. Compared with the control samples, the thermal conductivity values observed for RHA constitutions of 25%, 50%, 75% and 100% were approximately 7%, 11%, 22% and 28% lower, respectively, and these decreased values were related to the low dry density of the RHC samples. These results demonstrated that the porous structure and low specific gravity of RHA had led to a decrease in the heat transfer and thermal conductivity of RHC.

Table 5.1 Thermal conductivity of RHC.

Samples	Dry density (kg/m^3)	Thermal conductivity (W/mK)
CT	1219	0.3758
RHC25	1026	0.3487
RHC50	882	0.3325
RHC75	754	0.2927
RHC100	671	0.2670

5.4.3.4 Microstructural Analysis

The microstructures of the RHC samples and the control samples were examined using XRD and SEM combined with energy-dispersive spectroscopy (EDS). The XRD analyses were performed to identify the crystalline solid phases. The diffraction patterns are presented in Fig. 5.15 and Fig. 5.16 for the samples cured at a temperature of 180°C for 2 hr and 18 hr, respectively. Fig. 5.15 reveals the initial high intensity of the quartz peak and subsequent tobermorite and calcium hydroxide peaks for the control samples. When RHA was introduced, the intensity of the quartz peak was reduced, and the peak disappeared after 100% RHA substitution. In addition, the intensity of the tobermorite peak increased with increasing RHA dosages, while the calcium hydroxide peak disappeared as RHA was introduced. These results indicated that the high reactive silica in RHA quickly consumed the calcium hydroxide to form calcium silicate hydrate.

The SEM images illustrate that the fibrous CSH formed in the reference sample with 2 hr of autoclaving time (Fig. 5.17a-b) had been replaced by plate-like tobermorite at increased RHA replacement ratios of up to 50% (Fig. 5.17c). Further increases in the RHA replacement ratio led to the formation of crumbled foiled tobermorite and a following grass-like CSH structure with a very low Ca/Si ratio (Fig. 5.17d-e). Moreover, the SEM results also provided evidence of unreacted RHA on the surface when RHA was introduced. This effect may have caused the compressive strength reduction observed upon further RHA substitution during AAC production. With regard to the phase evolution of the $CaO\text{-}SiO_2\text{-}H_2O$ system during the hydrothermal reaction, the system contains over 20 crystalline phases [21], for example, tobermorite, xonotlite and jennite, and the formation of each of these phases depends on the autoclaving temperature and time and on the Ca/Si ratio [19]. However, for the above SEM results, the temperature and time were controlled at 180°C for 2 hr. Therefore, the Ca/Si ratio plays a significant role in determining the formation of crystalline phases. Typically, the optimum Ca/Si ratio for tobermorite formation is in the range of 0.8-1. Due to the low reactivity of quartz sand, the high concentration of quartz sand led to a high Ca/Si ratio (>1) and could not convert amorphous CSH to tobermorite at an early stage. A decrease in the Ca/Si ratio occurred when sand was substituted with the highly reactive RHA. This produced the tobermorite formation in the plate and crumbled foiled crystalline. However, the 100% RHA substitution for sand gains the Ca/Si under the limit and CSH with a grass-type structure was formed. Thus, this finding showed good agreement with both the XRD and compressive strength results for the produced RHC, where the utilization of RHA has the advantage of reducing the autoclaving time.

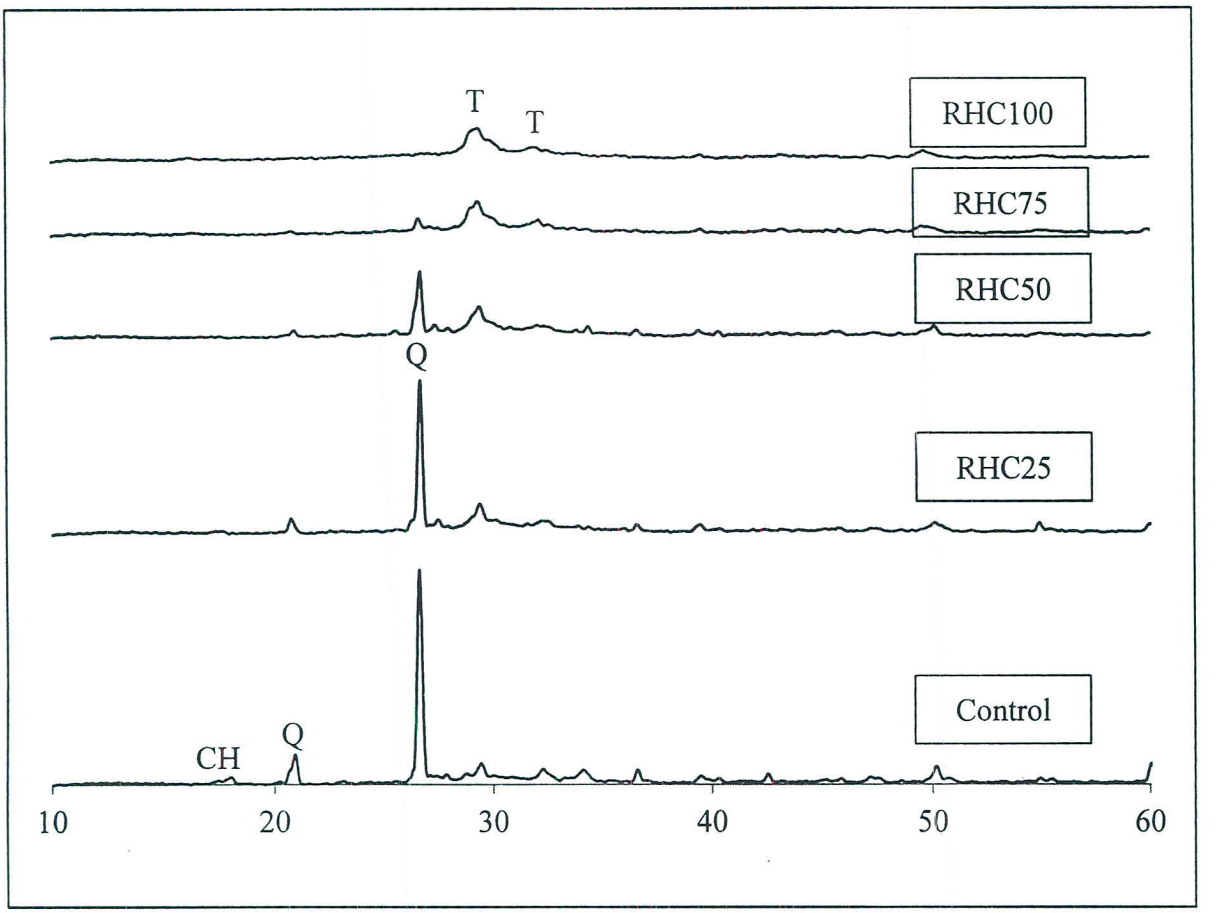

Figure 5.15 XRD pattern of autoclaved aerated concrete at 180°C for 2 hr. T: tobermorite; CH: calcium hydroxide; Q: quartz.

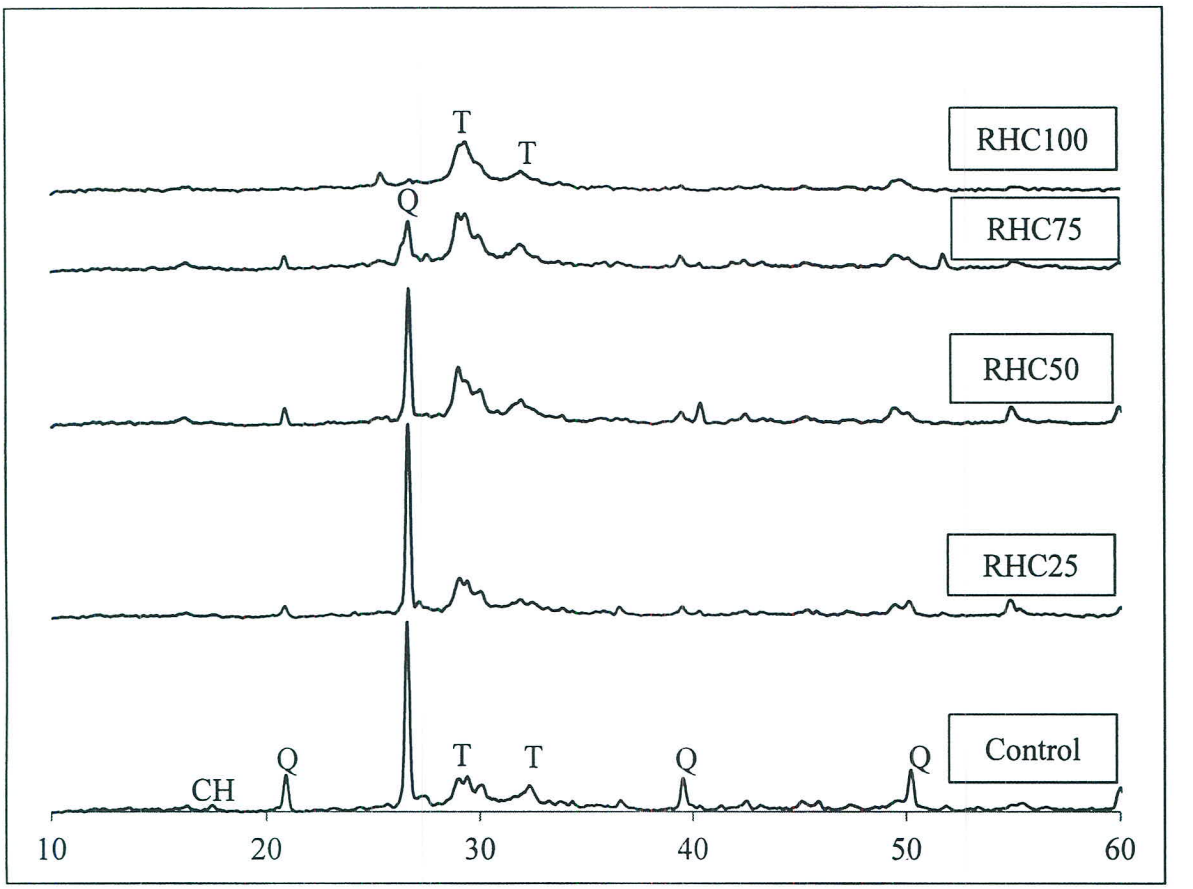

Figure 5.16 XRD pattern of autoclaved aerated concrete at 180°C for 18 hr. T: tobermorite; CH: calcium hydroxide; Q: quartz.

Nevertheless, an increased autoclaving time (18 h) found that needle-like tobermorite had formed in the reference sample (Fig. 5.18a) and changed to plate-like tobermorite in the presence of RHA (Fig. 5.18b). However, the increase in RHA substitution for sand had no significant effect (Fig. 5.18c-e). The crystalline structure changed in reference and RHC25 samples were due to the dissolution of quartz sand over time. This caused the Ca/Si ratio into the limit of tobermorite formation. Similar results were also observed by Mostafa (2005) [2], who used slag to replace sand with various lime contents and reported that, at a high lime content, the fibrous CSH was replaced by needle-like tobermorite with a long autoclaving time. In contrast with the low lime content samples, CSH with a glass-like structure was observed at 24 hr. Moreover, it has been reported that CSH formed with a Ca/Si ratio >1 tends to contain short silica chains in the early stage and is more easily transformed into tobermorite than CSH with a low Ca/Si ratio (i.e., <1) [21, 73, 74]. The stable crystalline structure of RHC samples occurred from

the reaction products, such as tobermorite, have a lower degree of decomposition than that of the starting materials. This shows that the reaction products became stable even through there was an increase in autoclaving time, when either of the starting materials is wholly consumed and the reaction is then in equilibrium [75]. In this study, energy dispersive spectroscopy (EDS) analysis revealed that the Ca/Si ratios of these types of crystalline phases were 1.28, 0.86, 0.85, 0.82 and 0.75 for CT, RHC25, RHC50, RHC75 and RHC100, respectively, as indicated in Table 5.2. Thus, the results of the present study agreed with the above findings.

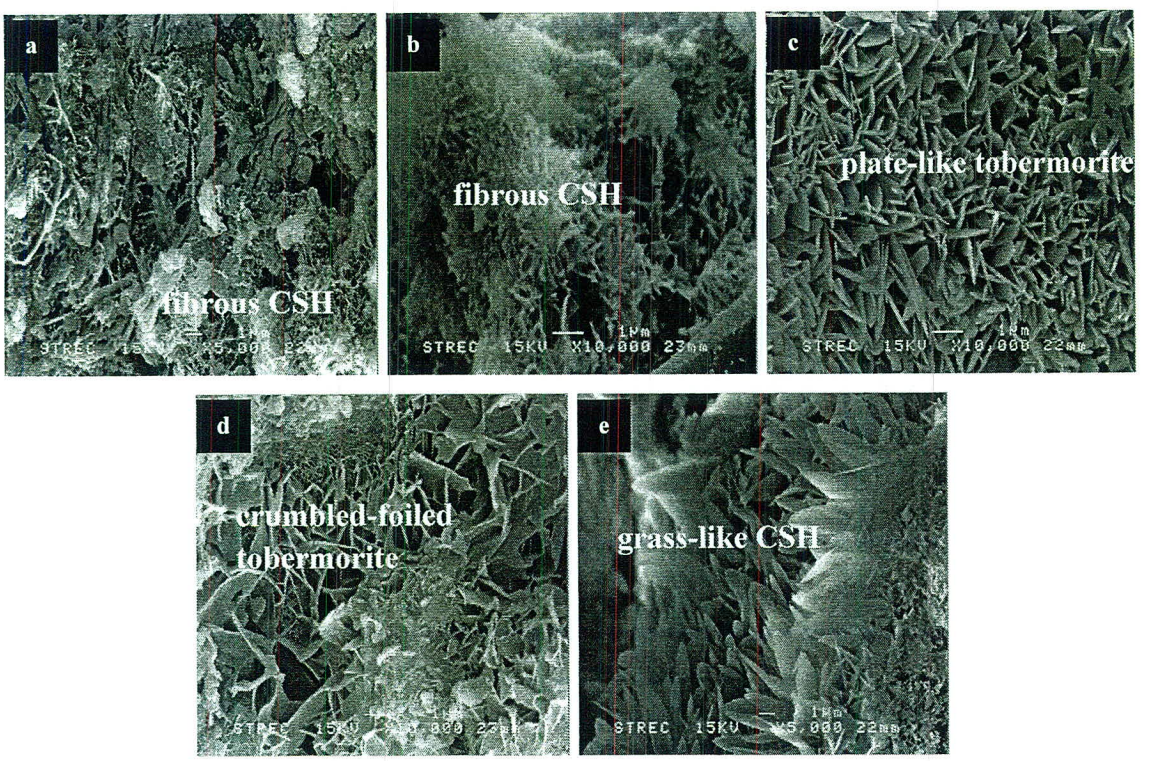

Figure 5.17 The morphology of AAC products at 180°C for 2 hr: (a) control, (b) RHC25, (c) RHC50, (d) RHC75 and (e) RHC100.

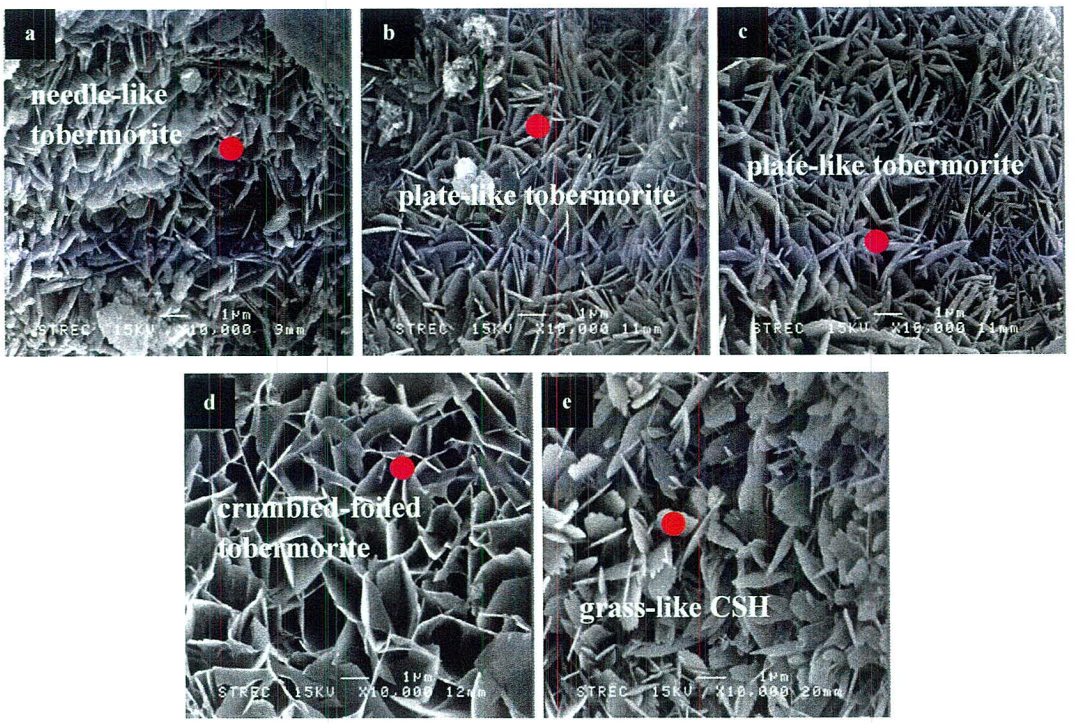

Figure 5.18 The morphology of AAC products at 180°C for 18 hr: (a) control, (b) RHC25, (c) RHC50, (d) RHC75 and (e) RHC100.

Table 5.2 Chemical analysis by SEM-EDS at 180°C for 18 hr.

Sample	Ca/Si	Ca/(Si+Al)	Al/(Al+Si)
CT	1.28	1.13	0.11
25	0.86	0.76	0.12
50	0.85	0.74	0.13
75	0.82	0.78	0.05
100	0.75	0.71	0.06

Both lower temperatures (140°C and 160°C) showed the crystalline peaks in XRD analysis to be similar to the samples prepared at a temperature of 180°C for all autoclaving times, as illustrated in Fig. 5.19-5.22. However, the intensity of the tobermorite peak at both 140°C and 160°C at all autoclaving times, except at 160°C for 18 hr, was found to be lower than those of the samples prepared at 180°C. These results contributed to the lower strength of the samples prepared at 140°C and 160°C.

Regarding the SEM technique, at a temperature of 140°C, the reference and the mixture incorporating RHA up to 75% contained the CSH in a fibrous and needle form at a short autoclaving time (Fig. 5.23a-d). The addition of further RHA content shows the plate-like tobermorite on the surface (Fig. 5.23e). With an increase in autoclaving time, the morphology was still found to be stable (Fig. 5.24a-e). This indicated that the low temperature of 140°C cannot convert CSH to tobermorite crystalline. Due to low degree of dissolution silicate anions at a low temperature, leads the Ca/Si ratio over the limit of tobermorite formation even though increasing autoclaving time. This finding shows good agreement on XRD analysis and compressive strength results. However, the remarkable aspect is that 100% RHA showed good pozzolanic materials in the hydrothermal reaction at a low temperature. From the above, the sand replacement by RHA gains a decreasing Ca/Si ratio. At a high temperature of 180°C, the Ca/Si ratio of RHC100 is under the limit on tobermorite formation. However, the lower degree of reaction at a low temperature has relatively low silica in solution compared with high temperatures and consequently has suitable Ca/Si ratio for tobermorite formation. Therefore, it can be recommended that the use of RHA in AAC production also reduces the autoclaving temperature.

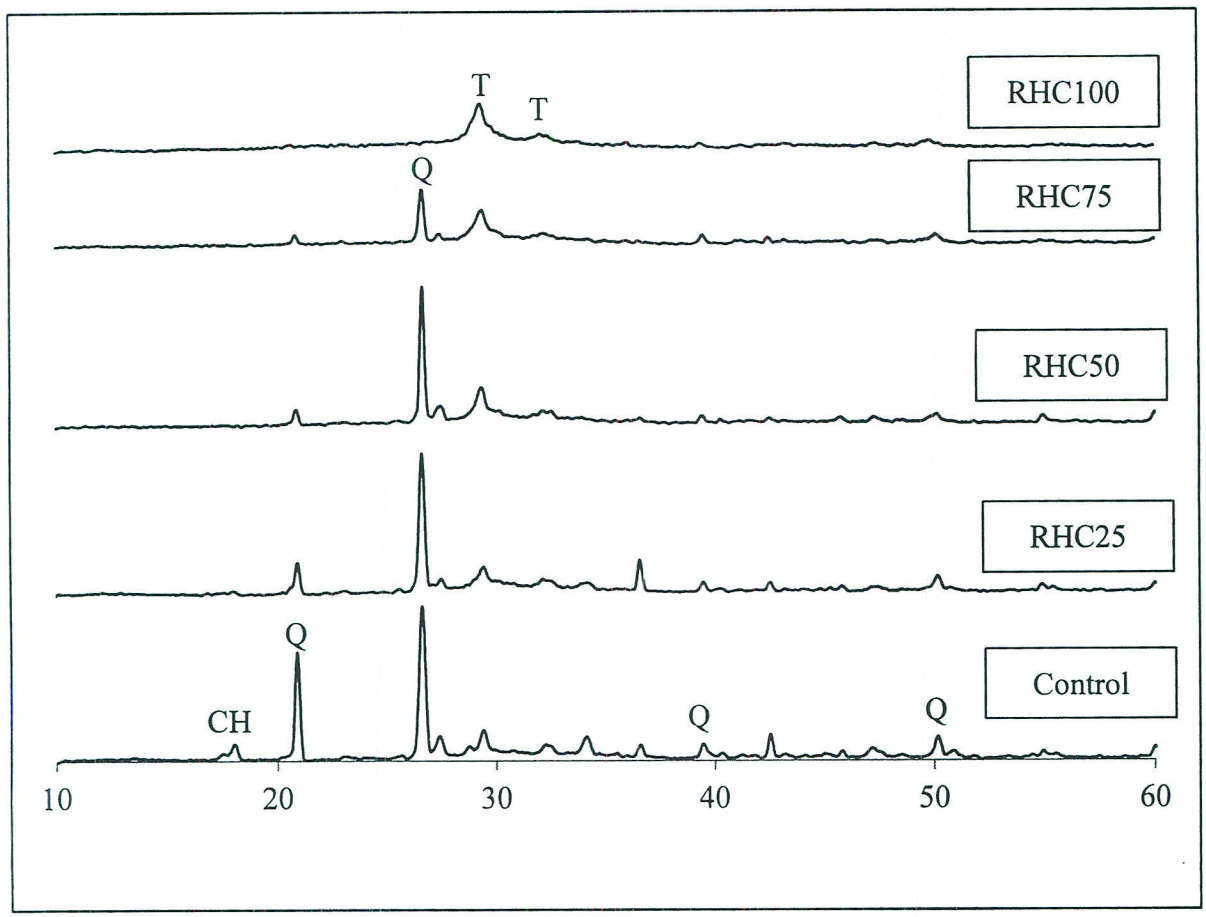

Figure 5.19 XRD pattern of autoclaved aerated concrete at 140°C for 4 hr. T: tobermorite; CH: calcium hydroxide; Q: quartz.

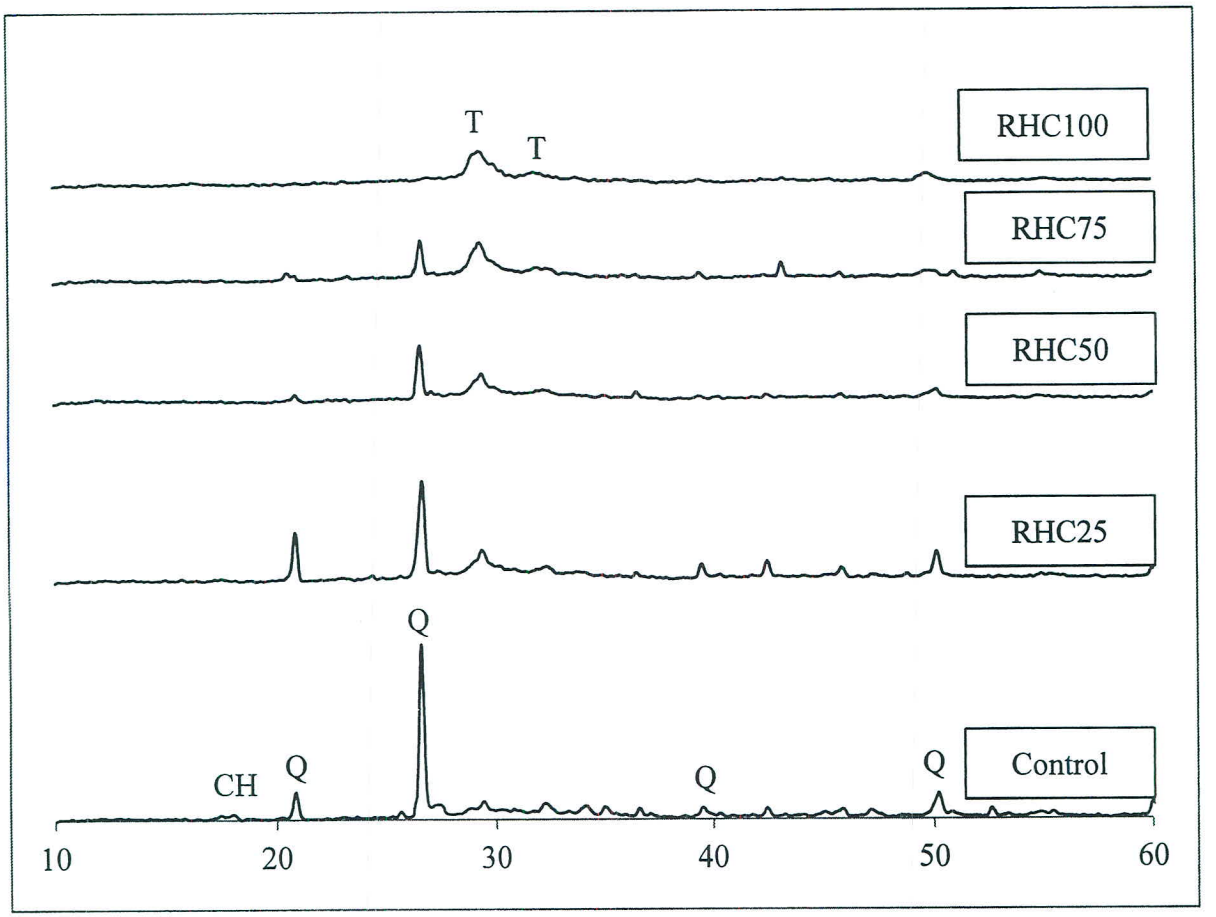

Figure 5.20 XRD pattern of autoclaved aerated concrete at 140°C for 18 hr. T: tobermorite; CH: calcium hydroxide; Q: quartz.

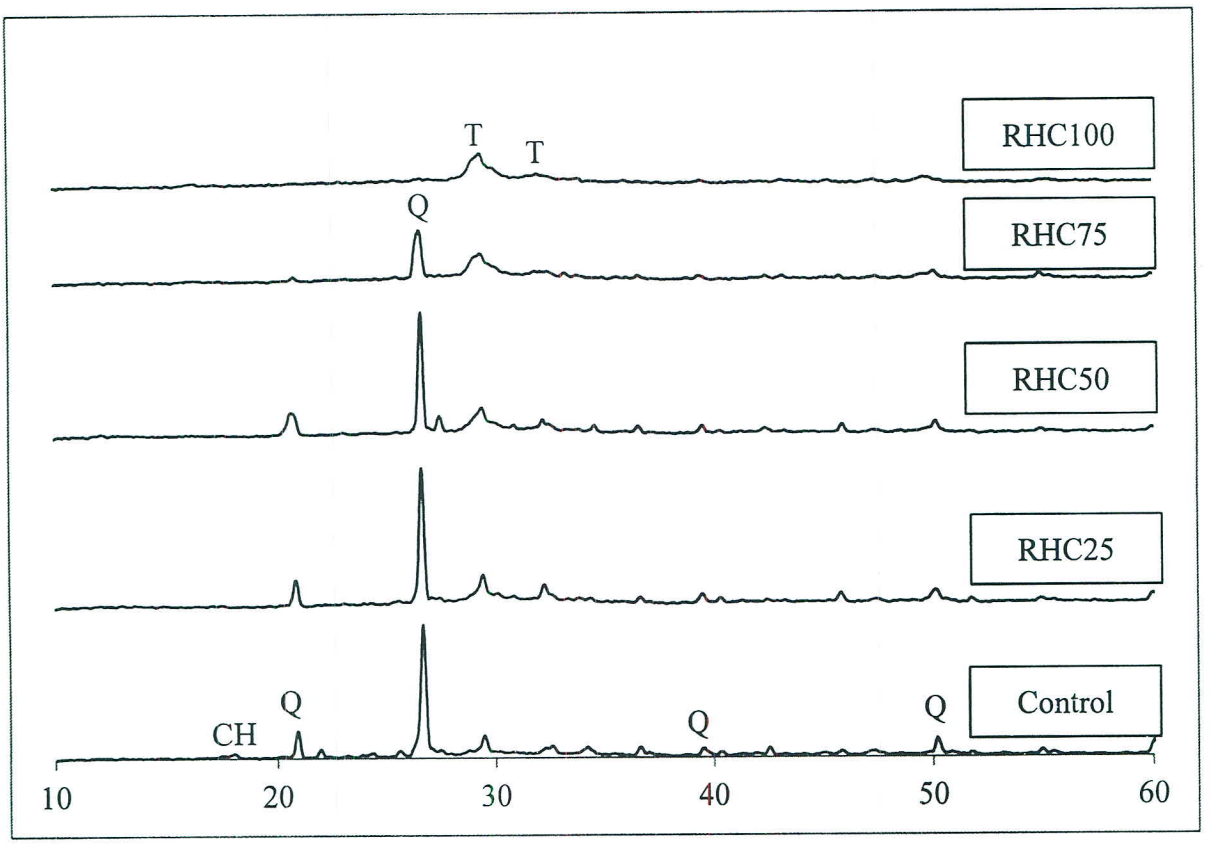

Figure 5.21 XRD pattern of autoclaved aerated concrete at 160°C for 4 hr. T: tobermorite; CH: calcium hydroxide; Q: quartz.

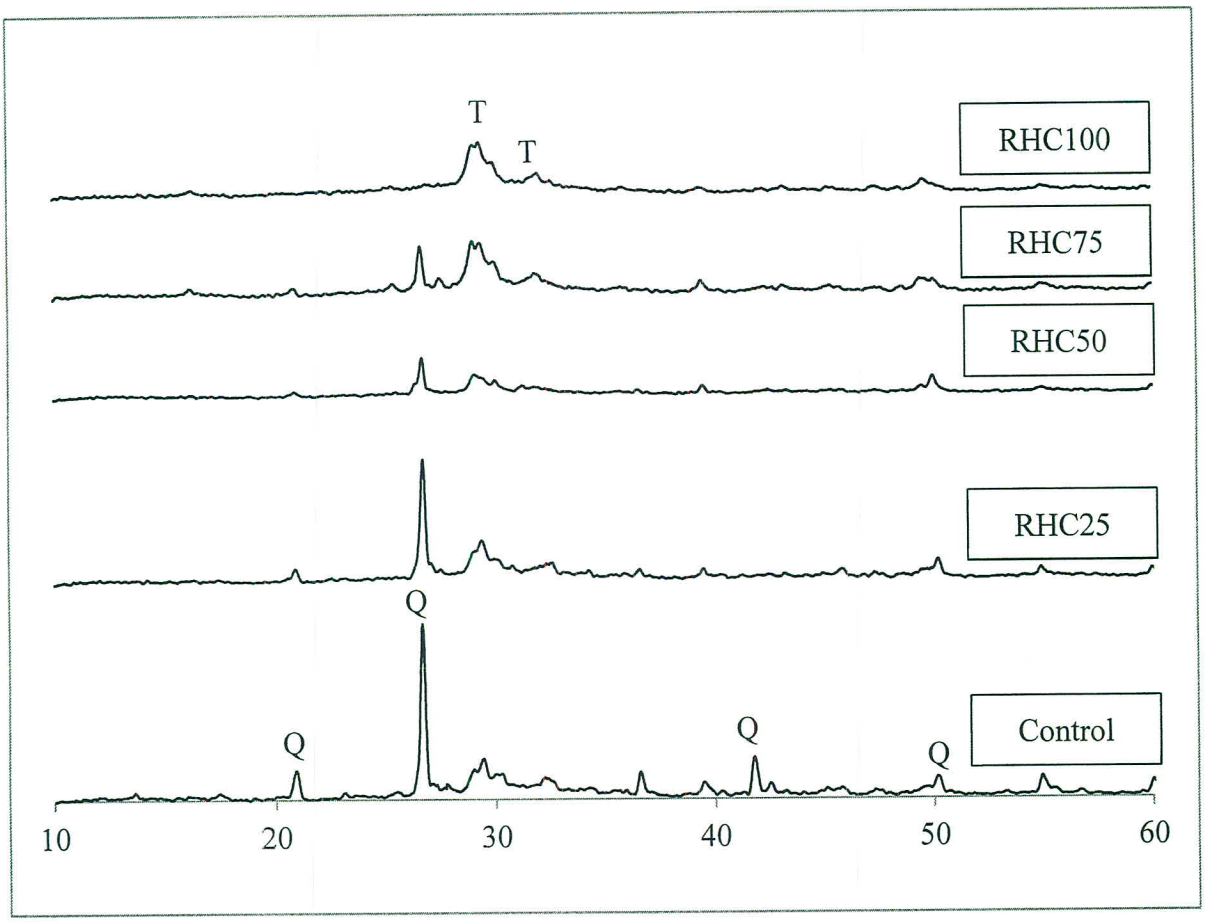

Figure 5.22 XRD pattern of autoclaved aerated concrete at 160°C for 18 hr. T: tobermorite; CH: calcium hydroxide; Q: quartz.

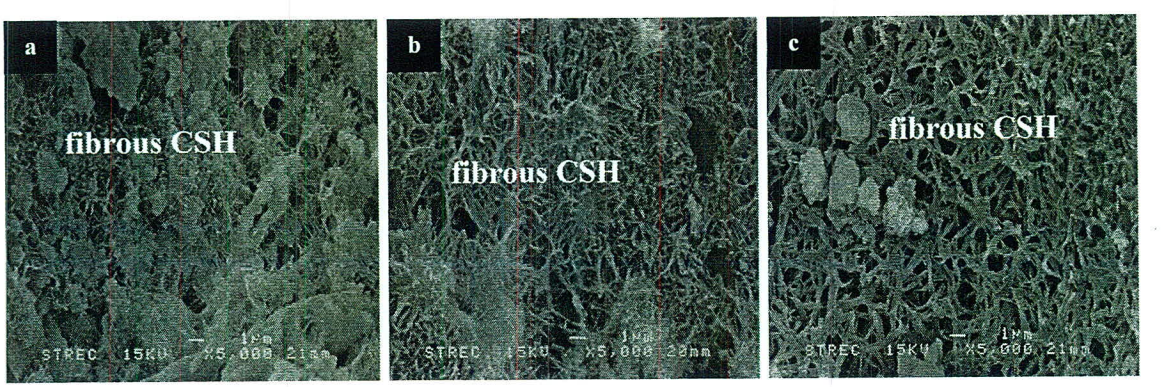

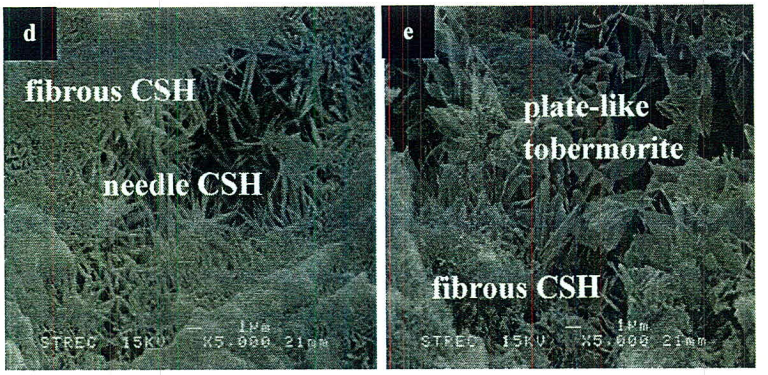

Figure 5.23 The morphology of AAC products at 140°C for 4 hr: (a) control, (b) RHC25, (c) RHC50, (d) RHC75 and (e) RHC100.

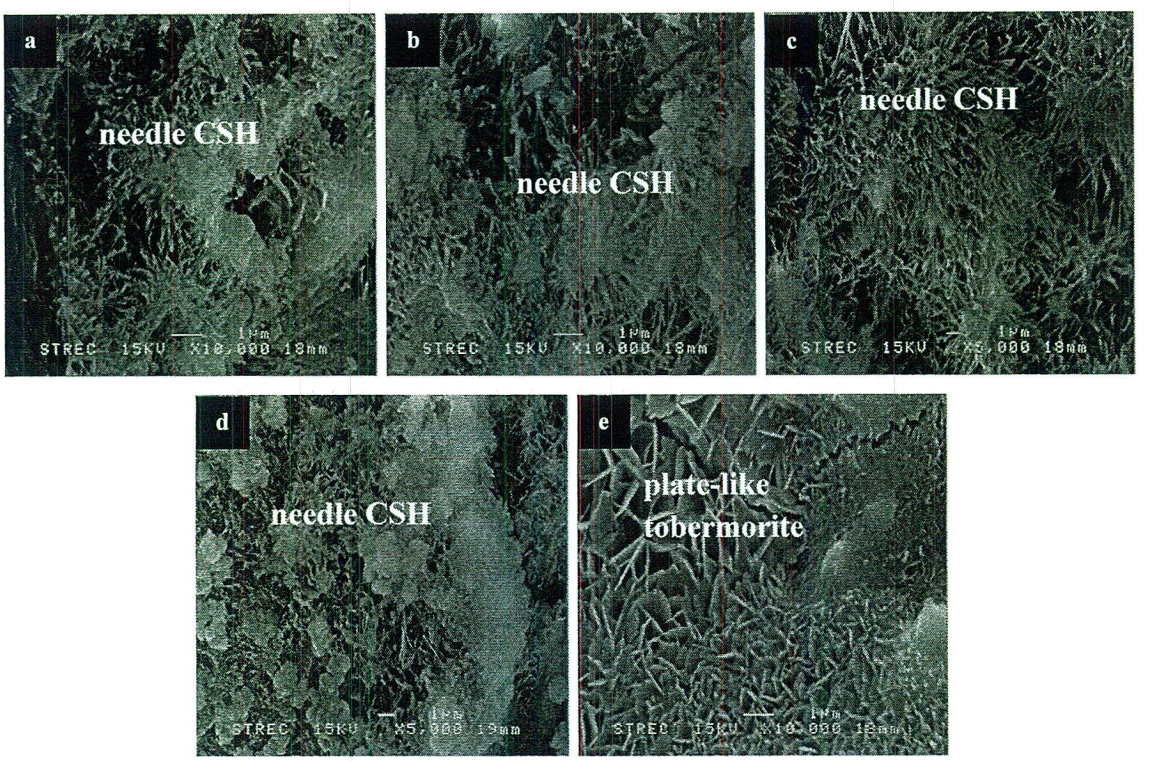

Figure 5.24 The morphology of AAC products at 140°C for 18 hr: (a) control, (b) RHC25, (c) RHC50, (d) RHC75 and (e) RHC100.

At a temperature of 160°C, the reference and RHC25 initially found the fibrous CSH (Fig. 5.25a-b), which changed to plate-like tobermorite with increasing RHA substitution for sand (Fig. 5.25c-d). The sand replacement by RHA at the level of 100% presents plate-like tobermorite and grass-like structure CSH with very low Ca/Si ratio.

However, the increase in autoclaving time tends to convert the fibrous CSH of reference, RHC25 and RHC75 to needle-like tobermorite, plate-like tobermorite and crumbled-foiled tobermorite, respectively. Similar results were obtained by Matsui et al. (2011) [58], who noted that the high reactivity of quartz presented a relatively higher intensity of tobermorite than that of low reactivity of quartz in the early stages. On the other hand, at the late stage, the intensity of tobermorite in low reactivity of quartz continued the increament, but a high reactivity of quartz became stable. Moreover, the reaction products at 160°C for 18 hr showed similar morphology with the samples prepared at 180°C for 18 hr. This confirmed that the strength values of samples prepared at 160°C for 18 h was equal to the samples prepared at 180°C for 18 hr. This indicated that the autoclaving temperature of 160°C for 18 hr can accelerate the degree of reaction of starting materials to produce reaction products into the equilibrium. This tends to show that the reaction of the starting materials is retarded and inhibited. However, at the same Ca/Si ratio (0.8-1) if the autoclaving temperature has increased above 180°C, the tobermorite crystalline begins to become unstable and can be transformed to xonotlite [19]. This brings strength loss.

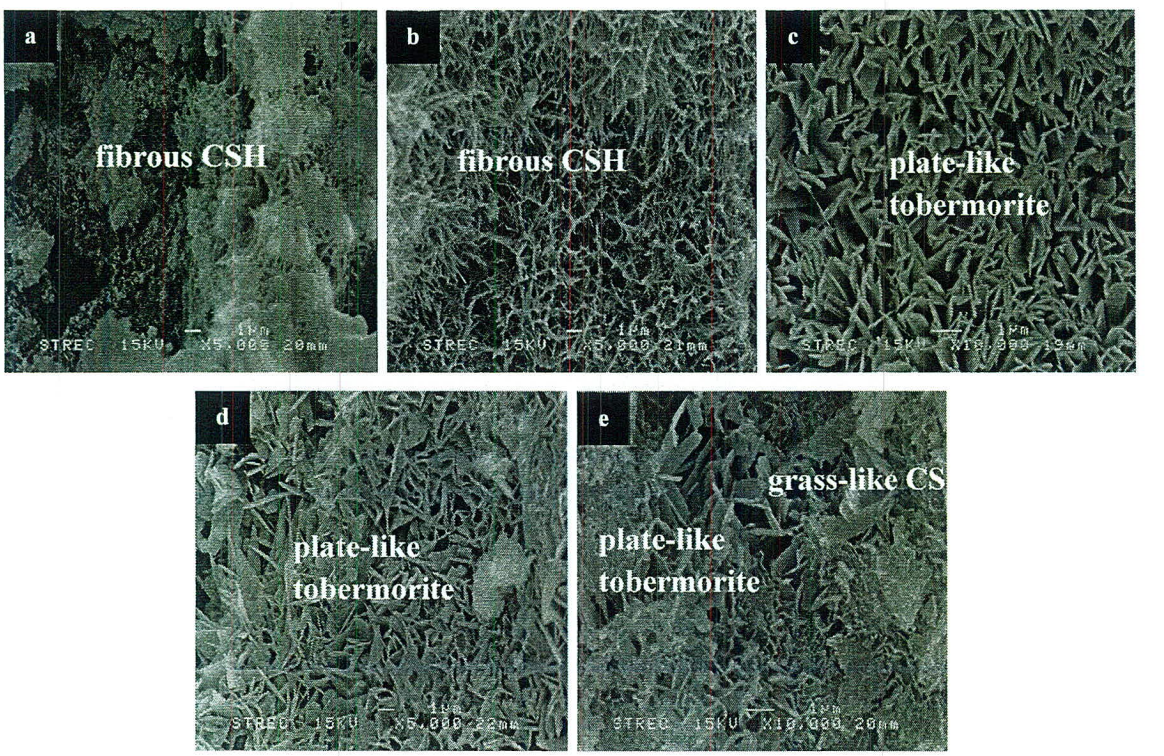

Figure 5.25 The morphology of AAC products at 160°C for 4 hr: (a) control, (b) RHC25, (c) RHC50, (d) RHC75 and (e) RHC100.

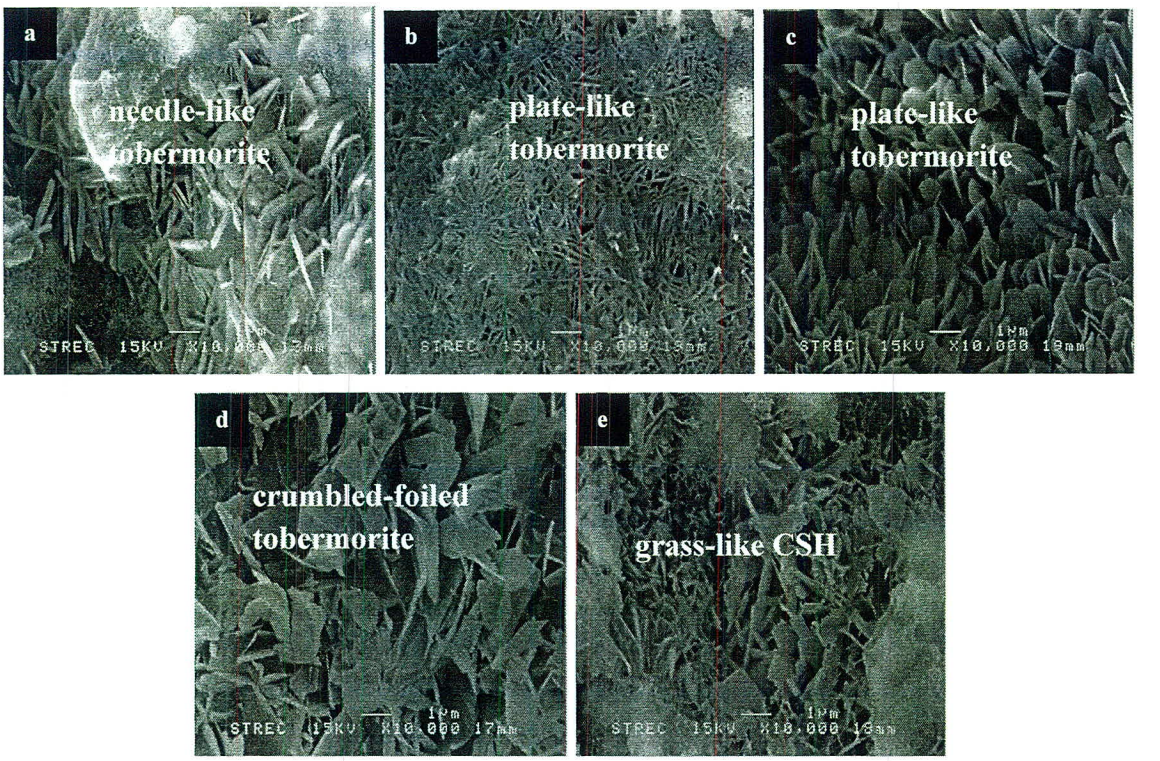

Figure 5.26 The morphology of AAC products at 160°C for 18 hr: (a) control, (b) RHC25, (c) RHC50, (d) RHC75 and (e) RHC100.

5.5 Conclusions

This study focused on the use of a readily available agricultural by-product, RHA, as a fine aggregate to replace sand in the production of AAC as well as the effect of curing conditions and autoclaving temperatures and times. The following conclusions can be drawn:

- The substitution of sand with RHA caused an increase in the water requirement, which negatively affected the compressive strength of the AAC. However, using RHA in AAC production also decreased the dry density.
- The autoclave curing tended to have more crystallinity of reaction products than the normal curing, which was revealed in the strength improvement.
- For RHA replacement levels of 75% and 100%, the compressive strength and unit weight values meet the ASTM C1386 standard limits for AAC-6 and AAC-4, respectively.

- The increase in temperatures and times has a positive impact on the degree of the reaction of the starting materials.
- As shown by the physical and mechanical results, the inclusion of RHA in AAC tended to decrease the required autoclaving time and temperature.
- With regards to the microstructure, high reactive silica was observed to have more of an effect on the transformation of CSH to tobermorite. A high level of silica leads to the formation of a glass-like CSH structure with a very low Ca/Si ratio.